

State dependent Riccati equation based filtering and control of a magnetorheological fluid brake

RENATO BRANCATI, RICCARDO RUSSO, MARIO TERZO

Dipartimento di Ingegneria Industriale
Università degli Studi di Napoli Federico II
Via Claudio 21, 80125, Napoli
ITALY
m.terzo@unina.it

Abstract – A theoretical/experimental activity has been carried out on a magnetorheological fluid brake prototype. A non-linear observer and an optimal control have been designed and tested on the physical device. Both the feedback control and the state observer are based on the state dependent Riccati equation technique. A first order non-linear dynamic model has been derived and adopted for the development of the braking torque control system. Simulation results confirm the goodness of the proposed control scheme which effectiveness has been evaluated by means of hardware in the loop tests.

Key-words: Measurement noise, Magnetorheological fluids, Kalman filter, Non-linear filtering and control.

1 Introduction

The property of the magnetorheological (MR) fluids of changing their rheological behaviour by means of an applied magnetic field allows them to be very useful as smart materials in controlled devices. MR fluid based devices have been under development since Rabinow employed them in the late 1940s [1]. In recent years, researchers have used the controllable variation in yield stress to develop various smart devices such as vibration dampers [2 – 8], transmission clutches [9 – 14], brakes [15 – 18] and automotive differential [19].

In this paper, a magnetorheological fluid brake (MRFB) torque control is designed and tested. The scheme of the controller is constituted by a combined action of feedforward and feedback control. The feedforward action is based on the resolution of the inverse dynamics, while the feedback contribution is designed employing the state dependent Riccati equation (SDRE) technique. Software simulations have been performed in order to highlight the goodness of the mixed control scheme and to confirm the MR fluid capability to be employed in control aimed devices. A hardware in the loop activity has been carried out on the MRFB prototype in order to evaluate the performances of the designed control of the braking torque. A SDRE based Kalman filter has been designed for the state measurement filtering in order to handle the noise

on the feedback signal.

2 The Magnetorheological Fluid Brake and Test Rig Description

The MRFB prototype, employed in the experimental activity, has been developed with reference to the morphology of a classical multi-plate viscous coupling. With reference to Fig. 1, the device consists of two series of discs (A) that are respectively integral with an internal rotor (B) and an external one (C). The two rotors are in relative motion. The discs are separated by spacer elements (D) in order to create a gap containing the MR fluid. The shear mode flowing typology takes place in the gap between the surfaces that are in relative motion. The magnetic field direction is at right angles to the direction of flow.

An external fixed casing (E) contains slots (F) for the positioning of 12 coils, each characterized by 30 turns.

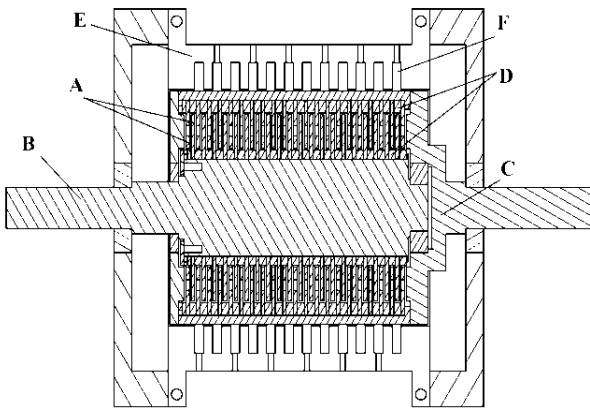


Fig. 1 Device cross section

Fig. 2 illustrates the two assembled rotors together with the input and the output shafts. The two coupled rotors are enclosed in the external fixed casing during the assembling procedure.



Fig. 2 The two coupled rotors

Fig. 3 shows the external casing, realized in two parts, and the coil.



Fig. 3 The coil

The device can be adopted as brake or clutch [19]. It can also act as an internal friction torque source if

integrated in a semi-active automotive differential [20]. The device characteristics are listed in Table 1.

Table 1 Device characteristics

Number of gaps containing MR fluid	40
gap outer radius	52 mm
gap inner radius	33 mm
gap height	1 mm

A careful selection of materials has been made in order to obtain the MR fluid magnetization. Aluminium has been adopted for the non-magnetic parts, while silicon steel has been used for the magnetic circuit components that are:

- the two series of discs;
- the external fixed casing;
- the two lateral flanges of the coupled rotors.

A finite elements analysis has been carried out to evaluate the intensity of the magnetic induction field. Fig. 4 illustrates the results obtained by “Maxwell®” (Ansoft) in presence of the adopted MR fluid (MRF 132DG by Lord Corporation) and a supply current of 6 A.

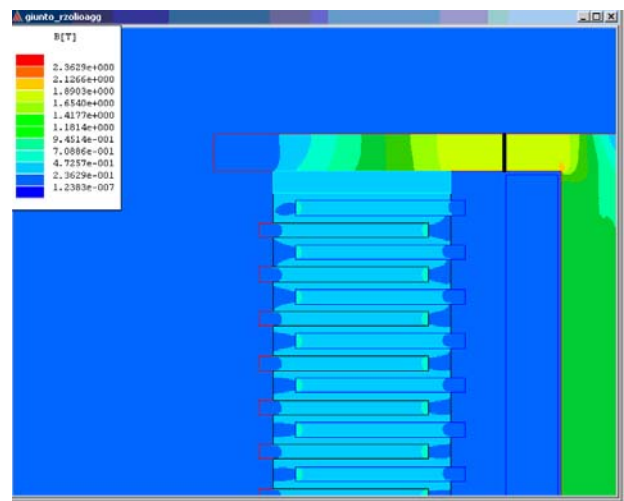


Fig. 4 Magnetic induction field

The magnetic induction appears sufficiently concentrated on the fluid located among the several discs.

Table 2 shows the MRF 132DG fluid characteristics.

Table 2 MR fluid characteristics

Properties	Value/Limits
Base fluid	Hydrocarbon
Operating temperature	-40 °C to 130 °C
Density range	2.95 to 3.15 g/cm ³
Color	Dark gray
Solids content by weight	80.98 %
Specific heat at 25 °C	0.71 J/g°C
Thermal conductivity at 25°C	0.28 – 1.28 W/m°C
Viscosity at 40°C	0.112 (± 0.02) Pa s

A suitable test rig (Fig. 5) has been realized in order to carry out experimental investigations. It includes the MR device (A), an inverter piloted electrical motor (B) and a dynamometric brake characterized by a rotor integral with the stator in order to create a pure fixed end. The rotational speed and the braking torque are measured.



Fig. 5 The test rig

3 Model Derivation

The MRFB is classified as a multi-input single-output (MISO) device. The inputs are constituted by supply current and rotational speed, whereas the output is the braking torque. The visco-plastic behaviour of the MR fluid can be modelled by the Bingham law:

$$\begin{cases} \tau_s \left(\frac{d\gamma}{dt}, H \right) = \tau_y (H) + \eta \frac{d\gamma}{dt} & \tau > \tau_y \\ \frac{d\gamma}{dt} = 0 & \tau < \tau_y \end{cases} \quad (1)$$

where τ_s is the shear stress, η the fluid

viscosity, $\frac{d\gamma}{dt}$ the shear rate, H the magnetic field and τ_y the yield stress.

According to the Bingham model, the transmitted torque is produced by two different contributions. The first one (T_v) consists of a viscous torque (Newtonian contribution) and the second one (T_m) depends on the MR fluid magnetization.

The whole device can be considered as the parallel of two branches, supplied by rotational speed and current respectively (Fig. 6).

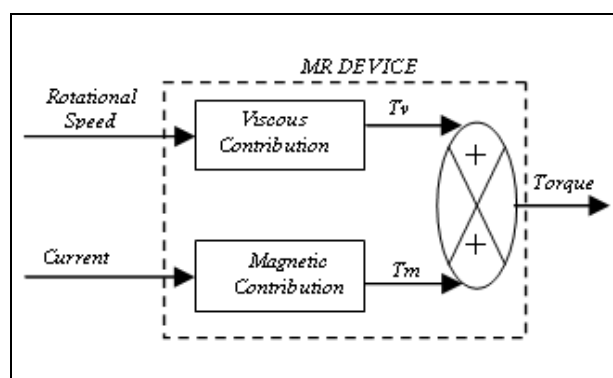


Fig. 6 Logical scheme of MR device

The first branch, related to rotational speed input, is modelled by the Newton viscous law. In fact, several experimental tests performed with no current input showed that, for the typical rotational speed employed, the relation between torque and velocity is purely algebraic, i.e. torque follows speed without appreciable lag.

Therefore, the relation between rotational speed and viscous torque is:

$$T_v = K_v(T_D) * \omega \quad (2)$$

in which ω is the rotational speed.

The branch supplied by the current (I) determines, as previously mentioned, the magnetic contribution (T_m). According to the literature, such a branch has been modelled as a first order system [21 – 24]. Fig. 7 illustrates the steady state T_m vs I characteristics, referring to constant values of both rotational speed and temperature.

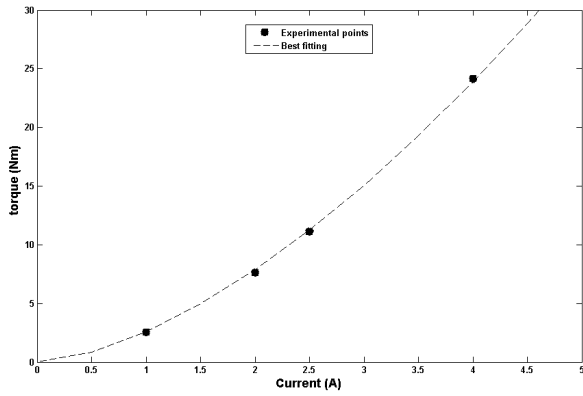


Fig. 7 Steady state T_m vs I dependence

The proposed fit for the steady state experimental result is:

$$T_m = K \cdot I^\rho \tag{3}$$

In order to define a state-space model characterized by the state variable T_m , the above steady state expression can be written as

$$T_m = K'(T_m) \cdot I \tag{4}$$

with:

$$K'(T_m) = T_m^{\frac{\rho-1}{\rho}} \cdot K^{\frac{1}{\rho}} \tag{5}$$

A state-space model providing the steady state response of (3) is:

$$\dot{T}_m = -\frac{1}{\tau} (T_m - T_m^{\frac{\rho-1}{\rho}} \cdot K^{\frac{1}{\rho}} \cdot I) \tag{6}$$

The equation (6) represents a state-space non-linear system that can be generically written as:

$$\dot{\mathbf{x}} = \mathbf{A}\mathbf{x} + \mathbf{B}(\mathbf{x})\mathbf{u} \tag{7}$$

Therefore, the complete system is modelled by the following set of algebraic-differential equations:

$$\begin{aligned} T_v &= K_v(T_D) * \omega \\ \dot{T}_m &= -\frac{1}{\tau} (T_m - T_m^{\frac{\rho-1}{\rho}} \cdot K^{\frac{1}{\rho}} \cdot I) \\ T &= T_v + T_m \end{aligned} \tag{8}$$

with K_v , K , ρ , and τ parameters to be

identified.

4. Control Design

The nonlinear model (8) has been adopted for the development of the braking torque control system.

The control action u is constituted by the current input. The control system is characterized by a mixed scheme (Fig. 8), in which a feedforward and a feedback contribution can be distinguished.

The feedforward control action u_{ff} is determined by solving the inverse dynamics of the open loop controlled system:

$$\dot{x} = Ax + B(x)u_{ff} \tag{9}$$

where

$$x = T_m$$

$$A = -\frac{1}{\tau}$$

$$B(x) = \frac{1}{\tau} (T_m^{\frac{\rho-1}{\rho}} \cdot K^{\frac{1}{\rho}})$$

T_m torque is obtained by subtracting the viscous torque T_v from the target one. Viscous torque T_v is estimated starting from the measured rotational speed and the identified K_v value.

A closed loop control action has been introduced in addition to the open loop one in order to compensate model and parameter uncertainty.

The feedback control has been developed using the state dependent Riccati equation. The SDRE technique is a non-linear control design method for the direct construction of non-linear feedback controllers [25 - 29]. Through the state dependent coefficient (SDC) factorization, system designers can represent the nonlinear equations of motion as linear structures with state dependent coefficients. Then, the LQ technique can be applied to this state dependent state space equation in which all matrices may depend on the states. The SDRE technique finds an input u_{fb} that minimizes the following performance index:

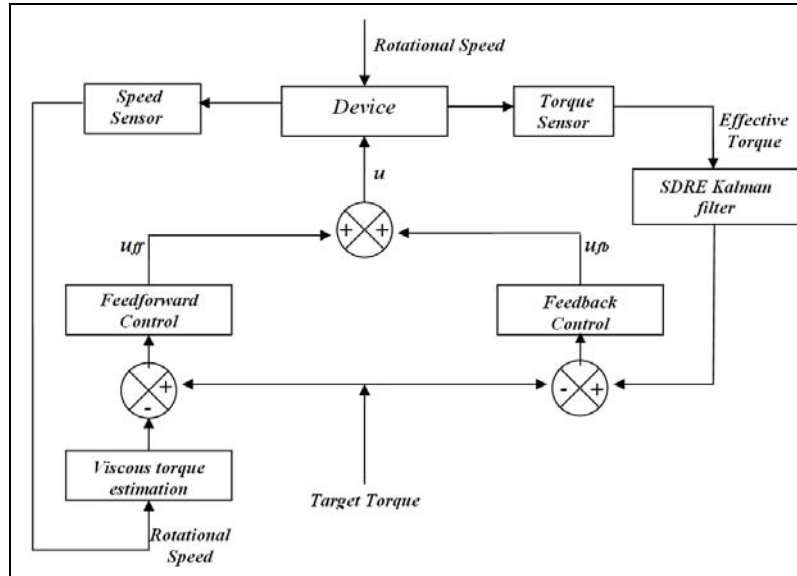


Fig. 8 Control scheme

$$J = \frac{1}{2} \int_0^{\infty} [x^{*T} Q x^* + u_{fb}^T R u_{fb}] dt \tag{10}$$

in which $x^* = x - x_T$ is the deviation between the real and the desired torque and

$$u_{fb} = -kx^*$$

$$k = R^{-1} B(x)^T P$$

P is the solution of the state-dependent Riccati equation

$$A^T P + PA - PB(x)R^{-1}B(x)^T P + Q = 0 \tag{11}$$

and Q, R the weight matrices to be matched experimentally.

5. The SDRE Kalman Filter

Because of the presence of a noisy feedback signal, the measured torque has been filtered by a SDRE based Kalman filter [30 - 32], improving the accuracy due to the non-linear nature of the system [33, 34]. The obtained signal has been then employed to supply the feedback state to the nonlinear optimal controller. A direct feedback of

the measured torque should cause a noise propagation on the control action and, therefore, a degraded controlled system response. At the same time, a typical low-pass filter cannot be employed because of the low frequencies that characterize the noisy signal.

In contrast to the linearized Kalman filter and to the extended Kalman filter, which are based on linearization, the SDRE Kalman filter is based on a parameterization that brings the non-linear system to a linear structure having state dependent coefficients (SDC). Taking into account the magnetic contribution of the MRFB in the SDC form

$$\dot{T}m = -\frac{1}{\tau} Tm - \frac{Tm^{\rho-1} K^{\rho}}{\tau} I \tag{12}$$

the SDRE Kalman filter is given by:

$$\dot{\hat{x}} = A\hat{x} + B(\hat{x})u_{fb} + k_k(y - C\hat{x}) \tag{13}$$

with

$k_k = P_k C^T R_k^{-1}$, and P_k solution of the state-dependent Riccati equation (14)

$$AP_k - P_k C^T R_k^{-1} C P_k + Q_k + P_k A_k^T = 0 \tag{14}$$

where \hat{x} is the filtered state, $C=1$ (state measurement), y is the torque measurement, Q_k and R_k are the process and the measurement white noise covariance matrices respectively.

The designed SDRE Kalman filter operates on the basis of system (6) and, starting from total torque measurement (y), supplies the filtered total torque employed as feedback signal for the nonlinear optimal control. It has to be considered that the purely algebraic nature of the viscous contribution allows to employ (6) as plant mathematical model for the non-linear feedback control and for the Kalman filter, both based on the SDRE technique. Indeed, the viscous contribution doesn't modify the actual plant dynamics and can be considered as a bias term for the MRFB torque which effects are minimized by means of the optimal approach employed for the feedback control and for the Kalman filter.

6. Simulation Results

The software results concerning the control performances are illustrated below. They refer to a constant rotational speed (600 rev/min). The initial condition of the plant is supposed to be equal to the viscous torque.

The identified parameters employed in simulations are illustrated in Table 3.

Table 3 Identified parameters

Parameter	Identified value
τ	0.04 s
K_v	0.035 Nms
K	2.11 Nm/A ^p
ρ	1.66

Fig. 9 and 10 represent the controlled system performance, in presence of a target torque of 15 Nm, and the control action respectively.

The results obtained for a constant target torque highlight the goodness of the developed control for both transient and steady state conditions.

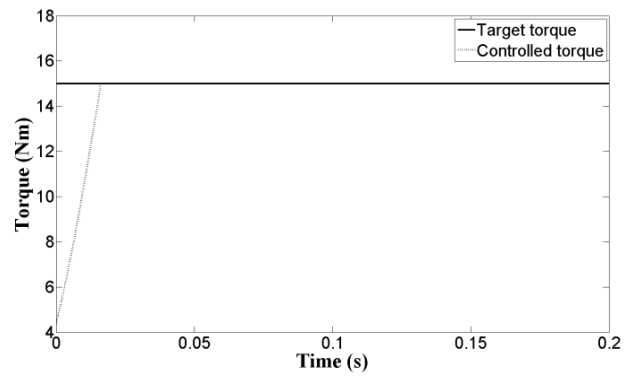


Fig. 9 Controlled system performance

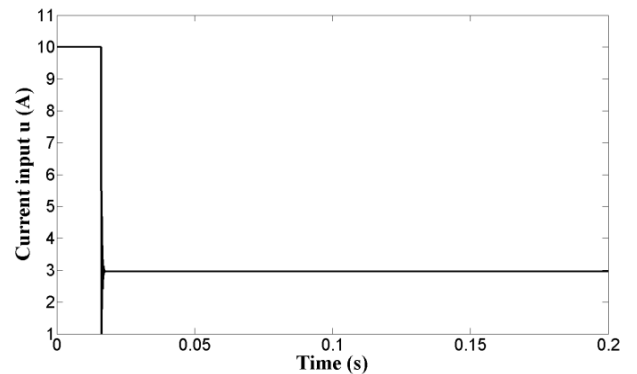


Fig. 10 Control action

In case of sinusoidal target torque (1 Hz), the system performance is represented in Fig. 11 and the control action in Fig. 12.

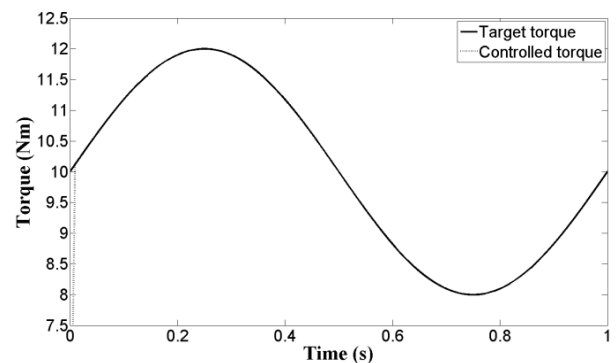


Fig. 11 Controlled system performance

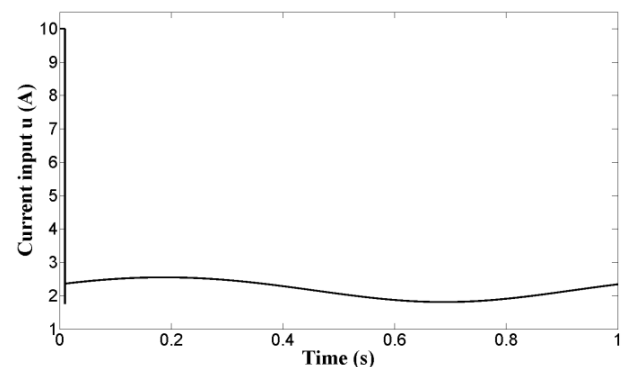


Fig. 12 Control action

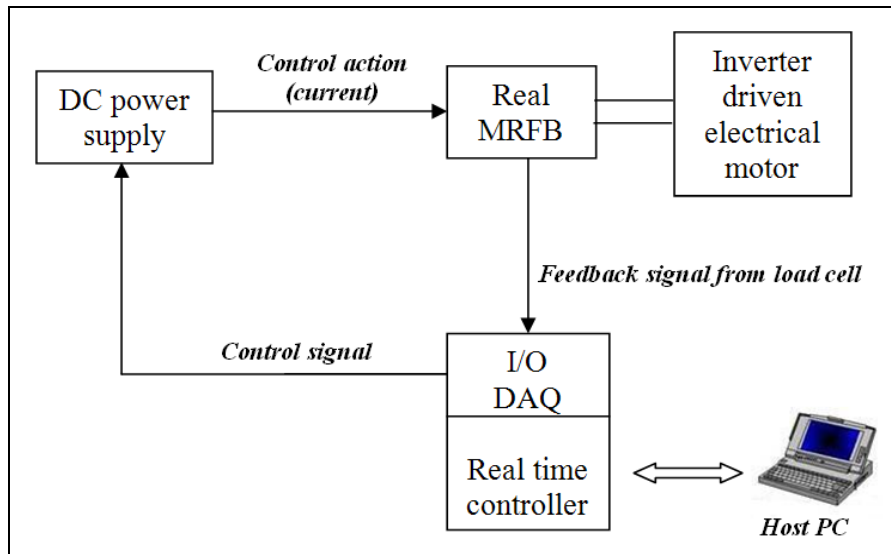


Fig. 13 HiL scheme

Also in presence of a sinusoidal time history for the target torque, the proposed control returns a good performance.

After having conducted software tests, an Hardware in the Loop (HiL) procedure has been realized and the results are presented in the following.

7. Experimental Results

In this section, the first tests concerning an HiL activity are described. The application is based on the real time control of the physical MRFB in order to realize the desired braking torque. The Fig. 13 represents the HiL scheme. The I/O DAQ receives the feedback signal from the load cell and, on the basis of the real time controller (NI CompactRIO) response, generates the control signal that drives a DC power supply. The generated current constitutes the control action for the MRFB that is characterized by a rotational speed of 600 rev/min by means of an inverter driven electrical motor.

The designed non-linear optimal control, coupled with the SDRE Kalman filter, has been tested in the hardware in the loop application. In the following, the test results are illustrated. Fig. 14 represents the performance of the controlled system in case of a constant target torque (15 Nm). The starting torque is obtained in absence of current input and, consequently, has to be ascribed to the viscous contribution only. Fig. 15 illustrates the obtained control action.

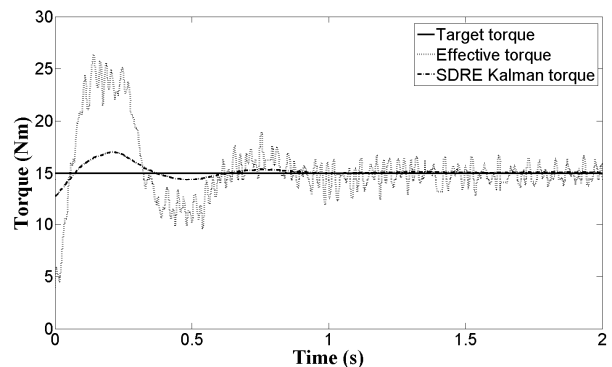


Fig. 14. Controlled system performance

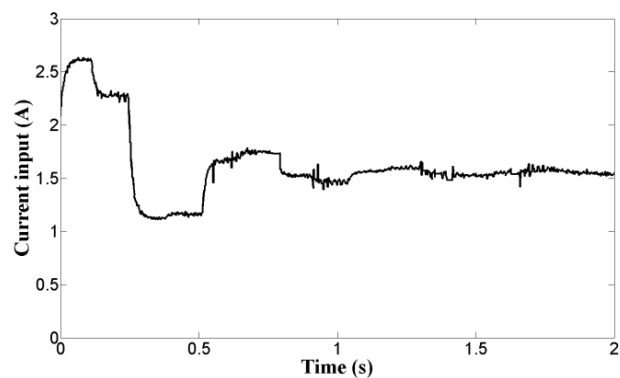


Fig. 15. Control action

The illustrated result highlights the capability of the designed control in presence of a constant target torque. The feedback of the SDRE Kalman filtered signal doesn't add noise on the control action. The estimation error ($y - \hat{x}$) causes a filtered torque value close to the real one. Such a difference is easily compensated by acting on the weight matrix Q associated to the deviation minimization (4). A

reduction of the estimation error could be reached by a reduction of the fixed step size employed in the computation procedure. This action has not been stressed in this results in order to avoid the increasing of the real time computational load.

It is interesting to note that, in the illustrated HiL results, the controlled MRFB exhibits a dynamic behaviour that has not been observed in the simulation results (Fig. 9, 11). It is caused by the presence of an extra current due to the electric circuit make which generates an overshoot of the MRFB torque. Moreover, HiL results show current values lower than the same illustrated in the simulations. It has to be ascribed to the greater viscous contribution (minor temperature) that characterizes the HiL tests.

Fig. 16 shows the controlled system performance in presence of a sinusoidal target torque characterized by a frequency of 1 Hz. The result confirms the control system effectiveness obtained by means of a control action illustrated in Fig. 17.

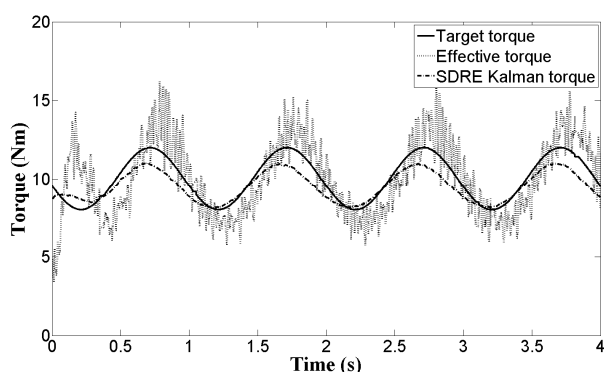


Fig. 16 Controlled system performance

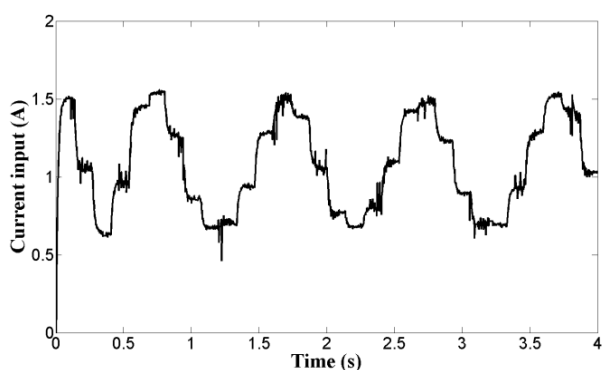


Fig. 17 Control action

The designed non-linear control, coupled with a SDRE Kalman filter, exhibits appreciable results in terms of tracking and noise handling also in presence of a variable target.

8. Conclusion

A theoretical/experimental activity has been carried out on a prototype of a magnetorheological fluid brake. The device is based on the shear mode flowing typology and is activated by the supply current.

A non-linear dynamic model has been derived and a non-linear optimal control, based on the SDRE technique, has been developed for the magnetorheological fluid brake. Software simulations confirmed the effectiveness of the proposed control and induced to employ it in an hardware in the loop application. The HiL activity has been carried out employing a SDRE based Kalman filter in order to handle the noise on the torque measurement.

The results have highlighted the goodness of the proposed control and have confirmed the MR fluid capability to be adopted in the control based applications.

References

- [1] Rabinow, The Magnetic Fluid Clutch, *AIEE Trans*, Vol. 67, 1948, pp. 1308 – 1315.
- [2] J.D. Carlson, D.N. Catanzarite and St KA Clair, Commercial Magneto-Rheological Fluid Devices, *Bullough W ed Proceedings 5th Int Conf on ER Fluids MR Suspensions and Associated Technology*, World Scientific Singapore, 1996, pp. 20–28.
- [3] M.R. Jolly and J.D. Carlson, A Controllable Squeeze Film Damper using Magnetorheological Fluid, *Proceedings of Actuator 96 Bremen GY*, 1996, pp. 333–336.
- [4] G.M. Kamath, N.M. Wereley and M.R. Jolly, Analysis and Testing of a Model-scale Magnetorheological Fluid Helicopter Lag Mode Damper, *J American Helicopter Soc*, Vol. 443, 1996, pp. 234–248.
- [5] N.M. Wereley and L. Pang, Nondimensional analysis of semi-active electrorheological and magnetorheological dampers using approximate parallel plates models, *Smart Materials and Structures*, Vol. 7, 1998, pp. 732-743.
- [6] B.F. Spencer Jr, G. Yang, J.D. Carlson and MK Sain, Smart Dampers for Seismic Protection of Structures: A Full-Scale Study, *Proceedings of the Second World Conference on Structural Control 2WCSC*, Vol. 1, June 28–July 1 Kyoto Japan, 1998, pp. 417–426.
- [7] G. Yang, Large-Scale Magnetorheological Fluid Damper for Vibration Mitigation: Modeling

- Testing and Control, *PhD Dissertation*, University of Notre Dame, 2001.
- [8] G. Yang, H.J. Jung and B.F. Spencer Jr, Dynamic Modeling of Full-Scale MR Dampers for Civil Engineering Applications, *US-Japan Workshop on Smart Structures for Improved Seismic Performance in Urban Region*, Aug 14–16 Seattle WA, 2001, p 20.
- [9] E.E. Bansbach, Torque Transfer Apparatus Using Magnetorheological Fluids, United States Patent Number 5779013, 1998.
- [10] S. Gopalswamy and G.L. Jones, Magnetorheological Transmission Clutch, United States Patent Number 5823309, 1998.
- [11] D. Lampe, A. Thess and C. Dotzauer, MRF-Clutch-Design Considerations and Performance, *The 6th International Conference on New Actuators*, Bremen, 1998.
- [12] J.D. Carlson, Low-Cost MR Fluid Sponge Devices, *Journal of Intelligent Material Systems and Structures*, Vol. 10, 1999, pp. 589–594.
- [13] D. Lampe and R. Grundmann, Transitional and Solid State Behavior of a Magnetorheological Clutch, *The 7th International Conference on New Actuators*, Actuator 2000 Bremen, 2000.
- [14] B. Kavlicoglu, N. Kavlicoglu, Y. Liu, C. Evrensel, A. Fuchs, G. Korol and F. Gordaninejad, Response time and performance of a high-torque magneto-rheological fluid limited slip differential clutch, *Smart Materials and Structures*, Vol. 16, 2007, pp. 149-159.
- [15] J.D. Carlson, Magnetorheological Brake with Integrated Flywheel, United States Patent Number 6 186290 B1, 2001.
- [16] K. Karakoc, E.J. Park, A. Suleman, Design considerations for an automotive magnetorheological brake, *Mechatronics*, Vol. 18, 2008, pp. 434-447,.
- [17] R. Russo, M. Terzo, Design of an adaptive control for a magnetorheological fluid brake with model parameters depending on temperature and speed, *Smart Materials and Structures*, Vol. 20, No. 11, 2011, 115003.
- [18] R. Russo, M. Terzo, Modelling, parameter identification, and control of a shear mode magnetorheological device, *Proc IMechE Part I: Journal of Systems and Control Engineering*, Vol. 225, No. 5, 2011, pp. 549 – 562.
- [19] R. Russo, M. Terzo, F. Timpone, Software-in-the-loop development and experimental testing of a semi-active magnetorheological coupling for 4WD on demand vehicles. *Proceedings of the Mini Conference on Vehicle System Dynamics, Identification and Anomalies*, 2008, pp. 73 - 82.
- [20] R. De Rosa, M. Russo, R. Russo, M. Terzo, Optimisation of handling and traction in a rear wheel drive vehicle by means of magneto-rheological semi-active differential, *Vehicle System Dynamics*, Vol. 47, No. 5, 2009, pp. 533-550.
- [21] N. Takesue, J. Furusho and M. Sakaguchi, Improvement of Response Properties of MR-Fluid Actuator by Torque Feedback Control, *Proc. of the International Conference on Robotics & Automation*, Seoul, Korea, 2001, pp. 3825 – 3830.
- [22] Y.J. Nam, Y.J. Moon, M.K. Park, Performance Improvement of a Rotary MR fluid Actuator based on Electromagnetic Design, *Journal of Intelligent Materials Systems and Structures*, Vol. 19, No. 6, 2008, 695-705.
- [23] O. Ashour, C.A. Rogers, W. Kordonsky, Magnetorheological fluids: materials, characterization and devices, *Journal of Intelligent Material Systems and Structures*, Vol. 7, No. 2, 1996, pp. 123 – 130.
- [24] W. Kordonsky, Elements and devices based on magnetorheological effect, *Journal of Intelligent Material Systems and Structures*, Vol. 4, No. 1, pp. 65 – 69, 1993.
- [25] T. Cimen, State-Dependent Riccati Equation (SDRE) Control: A Survey, *Proc. of the 17th IFAC World Congress*, Seoul, Korea, 2008, pp. 3761 – 3775.
- [26] T. Cimen, Systematic and effective design of nonlinear feedback controllers via the state-dependent Riccati equation (SDRE) method, *Annual Reviews in Control*, Vol. 34, pp. 32 – 51, 2010.
- [27] T. Cimen, Survey of State-Dependent Riccati Equation in Nonlinear Optimal Feedback Control Synthesis, *Journal of Guidance, Control, and Dynamics*, Vol. 35, No. 4, pp. 1025 – 1047, 2012.
- [28] S. Pagano, R. Russo, S. Strano, M. Terzo, Non-linear modelling and optimal control of a hydraulically actuated seismic isolator test rig, *Mechanical Systems and Signal Processing*, Vol. 35, No. 1 – 2, 2013, pp. 255-278.
- [29] S. Pagano, R. Russo, S. Strano, M. Terzo, Modelling and Control of a Hydraulically Actuated Shaking Table Employed for Vibration Absorber Testing. *Proc. of the ASME 11th Biennial Conference on Engineering Systems Design and Analysis (ESDA2012)*, Nantes, France, Vol. 1, 2012, pp. 651 – 660.
- [30] C.P. Mracek, J.R. Cloutier, C.A. D'Souza, A New Technique for Nonlinear Estimation, *Proc. of the 1996 IEEE International Conference on*

- Control Applications*, Dearborn, 1996, pp. 338 – 343.
- [31] N. Assimakis, D. Lainiotis, D. Ventzas, A Survey of Distributed and Decentralized Algorithms for the Solution of the Discrete Time Riccati Equation, ISSP, 2000.
- [32] N. Assimakis, D. Lainiotis, D. Ventzas, Centralized And Distributed Algorithms For The Solution Of The Discrete Time Riccati Equation. *World Multiconference on Systemics, Cybernetics and Informatics and 5th International Conference on Information Systems Analysis and Synthesis: Image, Accoustic, Speech and Signal Processing*, Vol.6, 1999.
- [33] Filippo Neri. Cooperative evolutive concept learning: an empirical study. *WSEAS Transactions on Information Science and Applications*, Vol. 2, No. 5, 2005, pp. 559-563.
- [34] José De Jesus Rubio Avila, Andrés Ferreyra Ramírez and Carlos Avilés-Cruz. Nonlinear System Identification with a Feedforward Neural Network and an Optimal Bounded Ellipsoid Algorithm, *WSEAS Transactions on computers*, Vol. 7, No. 5, 2008, pp. 542-551.